Quaternary Geochronology 72 (2022) 101343

Contents lists available at ScienceDirect

Quaternary Geochronology

journal homepage: www.elsevier.com/locate/quageo

Quartz luminescence sensitivity from sediment versus bedrock in highly weathered soils of the Piedmont of North Carolina, south-eastern USA

M.S. Nelson [a,*], M.C. Eppes [b], T.M. Rittenour [a,c]

[a] Utah State University Luminescence Laboratory, 1770. North Research Parkway, Suite 123, North Logan, UT, 84341, USA
[b] University of North Carolina-Charlotte, Department of Geography and Earth Sciences, 9201 University City Blvd., Charlotte, NC, 28223, USA
[c] Utah State University, Department of Geosciences, 4505 Old Main Hill, Logan, UT, 84321, USA

ARTICLE INFO

Keywords:
LM-OSL
Quartz sensitivity
Soil
Saprolite
Mobile regolith

ABSTRACT

Deeply weathered soils cover most of the Piedmont physiographic province of the south-eastern United States of America (USA). These soils have traditionally been inferred to derive from weathered bedrock, but recent work (e.g. Ferguson et al., 2019) suggests that deposited sediments are more prevalent than recognized. Distinguishing sediment from weathered bedrock is integral to understanding critical-zone processes and overall Quaternary landscape evolution, yet the well-developed, red, clay-dominated Ultisols of this temperate and humid region mask differences between transported from non-transported material. Our goal is to determine if optically stimulated luminescence (OSL) methods can distinguish quartz sand from allochthonous (e.g. transported sediment) versus autochthonous (e.g. *in situ* weathered bedrock) material in soil-profile and core samples from the Redlair Observatory in southwestern North Carolina, USA. Here, we turn to OSL sensitivity and linear-modulated OSL (LM-OSL) to observe the intensity or lack thereof of the fast-decay luminescence component (most light-sensitive signal) in quartz grains from soil horizons and crystalline bedrock-derived saprolite. We find that quartz grains sampled from *in situ* weathered bedrock as well as from saprolotized clasts of rock have weak luminescence properties and are not dominated by a fast-decay luminescence component. In contrast, quartz grains from transported sediment (e.g. mobile regolith; colluvium; alluvium) contain sensitive grains with more dominant fast components. These results suggest that quartz luminescence sensitivity can be a tool to differentiate between *in situ* weathered bedrock and similar looking mobile regolith and colluvium over-printed by soil development.

1. Introduction

The critical zone is the near-surface layer of the Earth that is shaped by processes involving interactions among living organisms, air, water, soil and rock. Given its ecological and economic importance, Critical Zone Observatories and other research sites have been established worldwide. These designated conservation and natural areas contain networks of distributed field stations out-fitted for high-resolution spatial and temporal data gathering spanning event to millennial time-scales and micro to macro spatial scales (e.g. meter-scale plots to large watersheds) (White et al., 2015). Societally important research at these study sites are linked to assessing how soil development/erosion, bedrock weathering and other critical-zone processes responded to past climate change, with a goal of better predicting response to current and future climate and land-use changes (e.g. Pelletier et al., 2015; Guo and Lin, 2016; Anderson et al., 2019). The bedrock-soil interface is highly relevant to understanding surface and near-surface processes (e.g. Lebedeva and Brantley, 2013; Rempe and Dietrich, 2014; Riebe et al., 2017), however, processes driving regolith production at depth can be difficult to quantify on large scales given the challenge of making direct subsurface observations. Thus, there is a need to find additional tools that can be used on rock and soil core samples to generate data needed to build better models of the complex processes at depth.

Physical and chemical weathering are the agents of change in an evolving soil-saprolite-bedrock profile, and methods employed to measure and observe these changes often involve aqueous, soil and rock geochemistry. Riebe et al. (2017) outline a detailed history of geologic investigations into deep critical zone processes which began as early as 1500 AD. Solute-based geochemistry of primary and secondary minerals is a long-standing tool used to characterize weathering flux at the

* Corresponding author.
E-mail address: michelle.nelson@usu.edu (M.S. Nelson).

https://doi.org/10.1016/j.quageo.2022.101343
Received 19 December 2021; Received in revised form 29 April 2022; Accepted 12 May 2022
Available online 23 May 2022

catchment scale (e.g. Velbel and Price, 2007). More specifically, soil geochemistry is used to define elemental mass transfer for quantifying losses and gains through down-profile chemical weathering and physical weathering of bedrock into saprolite, which is weathered rock that still retains its primary structures like foliation or mineral veins (Brimhall and Dietrich, 1987; Brimhall et al., 1991; Merritts et al., 1991). The challenge with this approach is that allochthonous particles can be included through downslope transport (e.g. hillslope sediment and colluvium) or distal-transport (i.e. eolian or alluvial sediment) processes, and/or soil materials may leave the system through gravity-driven processes. These fluxes could lead to a geochemical imbalance that is hard to trace due to exotic additions and/or unknown losses to the system.

Analysis of the quartz sand fraction from soil and saprolite sequences can provide added information about critical zone processes. For example, the concentration of cosmogenic radionuclides such as ^{10}Be within quartz minerals can be used to estimate soil formation, weathering and erosion rates (e.g. Pavich et al., 1985; Gosse and Phillips, 2001; Granger and Riebe, 2014). Innovative modeling of hillslope processes and downslope movement of sediment and soil (e.g. Furbish et al., 2018), and soil production are also possible with cosmogenic radionuclides (Heimsath et al., 1997; Heimsath and Korup, 2012). The challenge with utilizing cosmogenic nuclides is that they accumulate in soils over time and attenuate with depth, concentrations require calibration from atmospheric production rates, and modeling includes several assumptions related to soil density (Rodés and Evans, 2020) and/or steady state conditions (Román-Sánchez et al., 2019).

Luminescence properties of quartz provides another opportunity to test sediment provenance, transport processes and weathering/soil development. Optically stimulated luminescence (OSL) of quartz is typically used to date the last exposure of mineral grains to light or heat (Huntley et al., 1985) and the scale of observation ranges from single-grain (Duller, 2008) to small-aliquot (multi-grain) analyses (~2->100 grains per measurement). Luminescence intensity is variable from grain to grain and is dependent on intrinsic luminescence properties such as sensitivity/brightness (Preusser et al., 2006) and related but not limited to the geologic and sedimentary history (Sawakuchi et al. 2011, 2018; Simkins et al., 2016), environmental radioactivity (Durcan et al., 2015), and lattice defects within the quartz crystal (Götze, 2000). For use in geochronologic applications (Aitken, 1998), soils and pedogenically-altered parent material are typically avoided due to mixing of grains with different sunlight or high-heat exposure histories (e.g. Bateman et al., 2003), variation in the burial depth after deposition (e.g. Munyikwa, 2000), non-stationary radioactivity (e.g. Feathers, 2002), and fluctuations in groundwater level and porosity (e.g. Jeong et al., 2007).

Recent work incorporates luminescence data to better understand long-term landscape evolution. For example, Heimsath et al. (2002) use single-grain OSL on quartz sand from a hillslope in southeastern Australia to quantify soil mixing. The luminescence signal accumulated within re-buried quartz grains can be used to estimate time-averaged downward-velocity (Heimsath et al., 2002), and these rates become important along with supplemental utilities of the luminescence phenomena for modelling soil processes (Gray et al., 2019). Following this work, multi-grain and single-grain luminescence has been a reliable utility for: 1) examining mixed-dose distributions caused by bioturbation (e.g. Bateman et al., 2003, 2007; Forrest et al., 2003; Hansen et al., 2015; Kristensen et al., 2015), 2) calculating regolith production using apparent ages (e.g. Furbish et al., 2018), 3) measuring the number of surface-visited grains in a vertical profile (e.g. Reimann et al., 2017), and 4) identifying the population of grains from mobile regolith near the saprolite boundary along a soil catena with non-saturated feldspar infrared stimulated luminescence signals (e.g. Román-Sánchez et al., 2019). This body of work has led to a more detailed understanding of bioturbation processes and soil mixing over varying timescales and landscapes, though much less work has been applied to *in situ* sediment production from weathered bedrock and saprolite.

Quartz luminescence sensitivity (intensity of the luminescence signal per applied dose per unit mass) and signal components (fast-, medium-, and slow-decay as a result of stimulation) vary by rock type (e.g. Preusser et al., 2006; Sawakuchi et al., 2011, 2018; Guralnik et al., 2015), transport distance/sedimentary cycling (e.g. Moska and Murray, 2006; Fitzsimmons et al., 2010; Pietsch, 2008) and may also be related to weathering characteristics of the rock or saprolite (e.g. Jeong and Choi, 2012). Experimental and observational results suggest that transported sediment should be sensitized and have higher intensity fast-decay luminescence signals, while weathered bedrock and saprolite are expected to have weak luminescence signals dominated by slow-decaying (undatable) OSL components, although luminescence sensitivity might be enhanced with greater degrees of weathering (Jeong and Choi, 2012). We seek to expand on these ideas related to bedrock weathering by quantifying luminescence intensity from single grains and small-aliquots of quartz sand in samples taken from 1) unmistakably transported sediment (as evidenced by stratification and mobilized clasts) 2) clearly identifiable *in situ* weathered rock (as defined by the presence of primary metamorphic structures like foliation) and 3) from areas of soil profiles where the origins of the parent material are not evident. We investigate the LM-OSL signals from quartz grains derived from deep to shallow saprolite and overlying soil in the mature landscape of the Redlair Observatory in the Piedmont physiographic province of western North Carolina. This is an ideal area to investigate the luminescence properties of soil and saprolite sequences because of the pristine nature of the conservatory, allowing for clear observations of natural processes rather than heavily human-impacted soils covering much of the southeastern United States of America (USA).

Ultisols (highly-weathered, red, clay-dominated soils), saprolite, and weathered bedrock are ubiquitous in the Piedmont of the southeastern USA. Upland Piedmont soils in this region may contain alluvial and colluvial deposits and be expressed within inverted topography, where previously low-lying (depositional) areas are now at hillslope summits due to differential erosion (Pavich, 1989; Richter et al., 2020). Where gravel is absent, profiles with only fine-grained sediments show a similar appearance to residuum, or soil developed in weathered bedrock and saprolite (Ferguson et al., 2019). Distinguishing allochthonous (transported sediment) and autochthonous (*in situ* weathered) material in exposures of well-developed soil profiles can be challenging without geochemical or sedimentological analyses, particularly where the original bedrock texture is not evident in saprolite. Further, core samples often lack context needed to help distinguish weathered sediment versus bedrock due to limited observation widths of core segments. This paper offers recommendations for identifying transported sediment versus *in situ* weathered bedrock. Results demonstrate that OSL signals from quartz sand are sensitized in transported sediments and non-sensitized in saprolite. We measure the luminescence signals from quartz sand grains in soil-profile exposures from hand-dug pits where we can readily distinguish transported sediment versus bedrock, and then apply this same method to horizons where we are unable to distinguish these differences, including in core samples from summit landscape positions that lack exposure context. We test the hypothesis that transported colluvium will have more grains with fast-component dominated signals and overall higher magnitude luminescence intensity (photon counts per applied dose) than saprolite samples. We propose that this is due to the greater residence time and cycling of quartz grains at the Earth's surface from colluvial settings.

2. Field area

Our study area is located within the Redlair Observatory in southwestern North Carolina (NC), a uniquely well-preserved >2000-acre amalgamation of conservation areas. Historic and modern agriculture has been largely restricted to floodplains along the South Fork of the Catawba River because deeply incised tributary hillslopes preclude

large-scale farming. The Natural Resources Conservation Service (NRCS) has mapped three soil units within the study area (PaD2, PaE, CeB2) (Fig. 1). These well-developed Ultisol soils are distinguished based on their hillslope position, slope, and percent clay. The Redlair Observatory is a prime location for examining the properties of deeply weathered soils, mobile regolith, and saprolite to distinguish between these similar-appearing materials that are produced from different source-materials and modified by divergent processes.

The bedrock geology of the region includes highly-weathered igneous and metamorphic rock complexes that are folded and faulted late Proterozoic to early Paleozoic medium-grained felsic metavolcanic and intrusive rocks (Goldsmith et al., 1988). The eastern USA has been a passive tectonic margin since the breakup of Pangea (~180 Ma) and the Piedmont was not glaciated during the Quaternary. Located on the eastern flank of the Blue Ridge mountains, the Piedmont peneplain has been proposed to be in dynamic equilibrium where erosion, soil and saprolite production, and bedrock weathering actively shape landforms in this region (Pavich, 1989). Recent work suggests a more episodic landscape evolution (Richter et al., 2020), where inverted topography and transported sediments are located at some hillslope summits.

Three Ultisol soil series are present within the study area (Natural Resources Conservation Service, 2019). The Pacolet sandy clay loam (PaD2) contains 20–40% clay and is found on hillslopes along ridges and backslopes with a linear downslope profile and 8–15% slope gradients. The coarser Pacolet sandy loam (PaE) soils contain <20% clay and are found on interfluves and backslopes with convex downslope profiles with slopes 15–25%. The Cecil sandy clay loam (CeB2) contains 20–40% clay and is found in interfluves and summit landscape positions with convex downslope profiles and slopes of 2–8%.

Soil properties from six soil pits are detailed in Table S1, and details include: horizon name and depth, color, % gravel, texture, structure, clay films, consistency, boundary type, roots, pores, and other notable features. Master soil horizons in the Redlair soil pits are A, B, and Cr/Cg; nomenclature for soil horizons follow NRCS guidelines (Norton, 1939). The A soil horizon is the topmost layer that contains a mix of organic and mineral matter and depth is variable between soil pits, extending down to 12 cm. The B soil horizon is part of the subsoil and contains accumulated minerals and oxides weathered from higher in the soil profile. Clay-rich B horizons contain elevated translocated clay minerals (noted with a 'Bt'). The use of numbers before the master soil horizon letter (such as '2Bt') indicates a different parent material than the overlying horizons. Numbers after the soil-horizon label indicate different characteristics of the same-classified horizon above (for example '2Bt2'). C horizons denote relatively unweathered horizons; with 'Cr' used to identify weathered bedrock and saprolite, and 'Cg' labels indicating gleyed color (water-saturated reducing conditions) in the parent material.

3. Methods

Linear-modulated OSL (LM-OSL) is measured by increasing the wattage of the light emitting diodes (LEDs) (mW/cm^2 output) and is used to determine the characteristics and intensities of the luminescence components (Bulur et al., 2000). Risø calibration quartz, used to calibrate luminescence instruments worldwide, is an ideal example of a highly-sensitized sample, where high sensitivity was generated through laboratory treatments involving multiple steps of high-temperature annealing, solar/optical bleaching, and beta/gamma irradiation (Hansen et al., 2015). Fig. 2A shows LM-OSL results from five 2-mm small-aliquots (~10 212-250 μm grains per measurement) of Risø calibration quartz batch 106 after 5.5 Gray (Gy, Joule/kg) of laboratory beta irradiation. Fig. 2B uses the fit_LMOSL code from the Luminescence Package in R Studio (Kreutzer, 2021) to model the components that make up the sum LM-OSL curve. For the calibration quartz sample, most of the signal is produced in the first 60 s of stimulation out of 500 s (0–12% blue-green diode power, 0–6 mW/cm^2). This initial

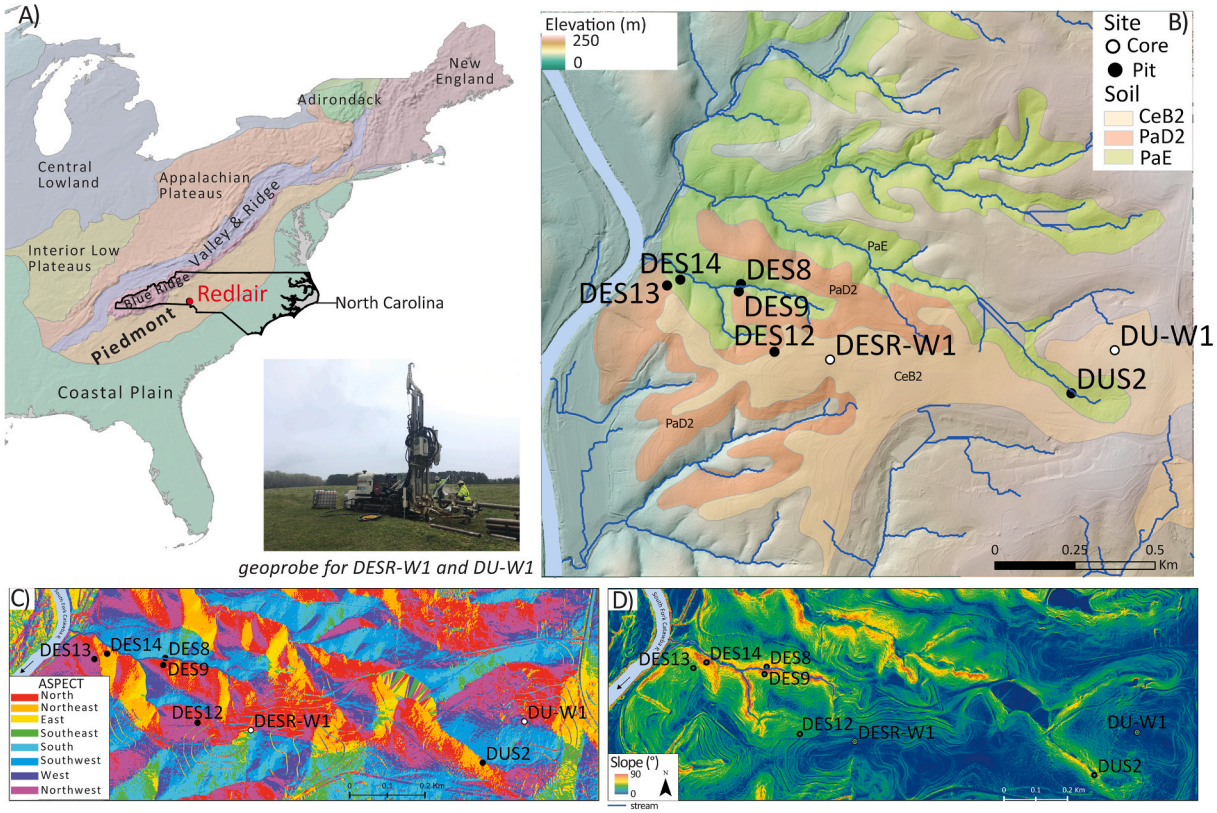

Fig. 1. A) Eastern USA physiographic provinces and location of Redlair Conservatory, NC. B) Hillshade and digital elevation model from 1-m lidar with overlay of soil polygons (USDA-NRCS) and core and soil pit locations. C-D) Aspect and slope derived from 1-m lidar dataset, respectively.

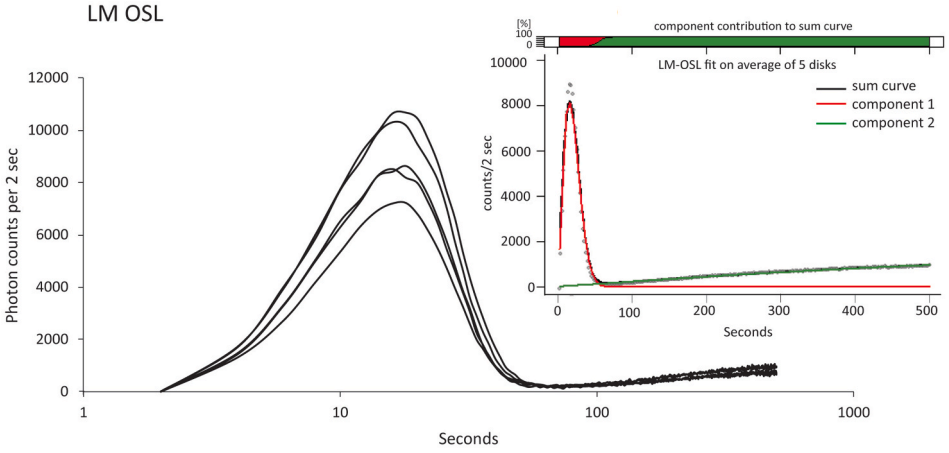

Fig. 2. Linear-modulated OSL (LM-OSL) of laboratory-sensitized Risø calibration quartz batch 106 after 5.5 Gy of beta irradiation given during regenerative dose step (Murray and Wintle, 2000). Results from five 2-mm small-aliquot disks of 180–250 μm quartz sand, measured over 500 s and 250 channels (background subtracted). Inset: Fit_LMOSL code from the Luminescence Package in R Studio to model the three components that make up the sum LM-OSL curve (Kreutzer, 2021).

luminescence signal emitted is called the fast component (Bailey et al., 1997). The medium and slow-decaying components are stimulated with higher intensity LED wattage (Fig. 2B). These slower-decaying components are not utilized for OSL dating because of their slow bleachability and/or thermal instability (e.g. Moska and Murray, 2006). However, these signals may be explored for understanding the provenance of mineral grains and their history of sunlight-heat-radiation exposure due to weathering and sediment transport (Sawakuchi et al., 2018). The intensity of the fast-component and total sensitivity has been linked to fluvial transport distance (e.g. Sawakuchi et al., 2011), geologic and sedimentary history (Sawakuchi et al., 2011, 2018; Simkins et al., 2016), environmental dose rate (Durcan et al., 2015), and/or mineral lattice defects and chemical impurities (Lain and Roberts, 2006).

3.1. OSL samples

Drainage divides and interfluves in the Piedmont often lack natural soil exposures given the rolling nature of the topography, vegetation cover, and the ubiquitous deep weathering profiles. Regolith depths in these upland landscape positions are 15 m thick or more, much greater than what is found on steep hillslopes (Pavich, 1989; Holbrook et al., 2014). Due to the landscape position and consequent depth to bedrock, soil cores were employed to sample the weathering profiles for OSL signals. We investigate six OSL samples from two >20 m deep geoprobe cores drilled at the South Fork of the Catawba River drainage divide (Fig. 2). Soils at the drilling locations are located within the CeB2 map units (Natural Resources Conservation Service, 2019), and parent material is saprolite derived from medium to high-grade metamorphic rocks. The Deep-South Rhyne well (DESR W1) was drilled on a first-order watershed interfluve summit and three OSL samples were collected from the ~21-m core (USU-3059 [0.91-0.97 m], -3060 [16.4 m], -3061 [16.5 m]). The Duffy Creek well (DU W1) was drilled at the summit of a major drainage divide between the ~7th-order South Fork of the Catawba and Catawba Rivers, ~0.75 km to the east of DESR W1 (Fig. 2). Three OSL samples (USU-3056 [0.66-0.71 m], -3057 [5.8-5.9 m], −3058 [24 m]) were collected from this ~24-m deep core (see Nelson et al., 2019 for core sampling details).

Six soil pits were dug in a range of geomorphic hillslope positions and slope angles. These soil pits exhibit differing degrees of chemical and physical weathering and soil development. Table 1 outlines the soil type and soil horizon of the OSL samples collected from the soil pits. Additional soil descriptions and details are available in Table S1. Twenty-six OSL samples were collected by pounding metal tubes into the six soil pits at a resolution of 3–6 samples from each pit (Figs. 3 and 4). In summary, the DES14 soil pit is 0.75 m deep and dug into a nearly flat in the floodplain of the South Fork of the Catawba River. The parent material is alluvium and no saprolite is present at the base of the pit. The DES13 soil pit was dug into a steep hillslope. This soil pit was 1.1 m deep, with saprolite developed in granodiorite parent material in exposed at the base of the pit, overlain by sediment/colluvium. DES9 and DES8 are a pair of soil pits located across from each other on backslope positions within a steep first-order valley; DES9 is north-facing and DES8 is south-facing. Both have saprolite exposed at the base of the 1.2–1.3 m deep pits and the parent materials are meta-volcanics overlain by sediment/colluvium. The DUS2 and DES12 soil pits were 1.07 and 0.9 m deep respectively and were dug into relatively shallow backslopes. No bedrock or foliated/textured saprolite is visible at the base of these pits and their bedrock type is not known. An intact quartz dike is present in DES12 suggesting this horizon may be highly-weathered saprolite/parent material. These two soil pits have B horizons with translocated clays (illuviation) and possibly colluvium.

3.2. OSL sample processing

Thirty-two OSL samples were processed and analyzed at the Utah State University Luminescence Laboratory in Logan, Utah, USA. Samples were opened under dim darkroom lighting (sodium vapor lamp, ~590 nm) and wet sieved. The 150–250 μm fraction was then treated with 10% hydrochloric (HCl) acid to remove post-depositional carbonate coatings and other acid-soluble salts for at least 24 h. Following a thorough rinse, 3-5% hydrogen peroxide (H_2O_2) or household bleach was added for at least 24 h to remove organic-rich material from the sieved fraction. Quartz minerals were isolated using water-soluble sodium polytungstate ($\rho = 2.72$ g/cm^3) and etched in 48% hydrofluoric (HF) and 30% hydrochloric (HCl) to remove feldspars, etch the outer few micrometers of the quartz grains to remove alpha doses and surface impurities such as iron oxides. Concentrated HCl was used to prevent the formation of fluorite precipitates during HF acid digestion.

3.3. OSL measurements

Quartz LM-OSL measurements were performed on Risø TL/OSL DA-20 readers. All 32 samples were first measured using small aliquots of sand to characterize the luminescence sensitivity and signal components of the soil, regolith and saprolite samples. Four 2-mm aliquots (~8-12 grains) were measured per sample, and the average signal of the four aliquots was used in the LM-OSL plots below. The natural dose was removed with continuous-wave OSL (CW-OSL) through optical bleaching with blue LEDs (470 ± 30 nm) for 40 s at 70% power (56 mW/cm^2). The aliquots were given a 22 Gy beta dose using a ^{90}Sr/^{90}Y beta source

Table 1
Soil pit samples and context.

Soil Pit	USU-#	Depth (cm)	Horizon	Context	Parent material
DES14 floodplain [PaE soil]	–	0–12	A	topsoil	alluvium
	USU-3278	12–24	AB	soil (eluvial)	alluvium
	USU-3279	24–38	BCg	soil	alluvium
	–	38–55	CgB	soil	alluvium
	USU-3280	55–74	2Cg	soil	coarse alluvium
DES13 23° hillslope [PaD2 soil]	USU-3281	0–7	A	topsoil	colluvium
	–	7–24	AB	soil (eluvial)	colluvium
	USU-3062	24–67	B	soil (illuvial)	colluvium
	USU-3063	67–92	2B	weathered saprolite	granodiorite
	USU-3064	67–92	2BCr	saprolite - original texture	granodiorite
	USU-3065	92–110	2CrB	saprolite - original texture	granodiorite
DES9 29° hillslope north-facing [PaD2 soil]	USU-3271	0–9	A	topsoil	colluvium
	USU-3272	9–22	AB	soil (eluvial)	colluvium
	USU-3070	22–32	B	soil (illuvial)	colluvium
	–	32–50	1/2B	soil (illuvial)	colluvium + metavolcanic
	USU-3071	50–87	2Bt	soil	metavolcanic
	USU-3072	50–87	2BtCr	saprolite clast	metavolcanic
	USU-3073	87–122	2BtCr2	saprolite	metavolcanic
DES8 27° hillslope north-facing [PaE soil]	USU-3273	0–9	A	topsoil	colluvium
	USU-3274	9–21	A/B	soil (eluvial)	colluvium
	USU-3067	21–48	2B	soil	metavolcanic
	USU-3066	48–92	2BtCr	soil	metavolcanic
	USU-3068	48–92	2BtCr	saprolite clast	metavolcanic
	–	92–112	2BtCr2	saprolite	metavolcanic
	USU-3069	112–131	2BCr	saprolite	metavolcanic
DUS2 10° hillslope [PaE soil]	USU-3268	0–11	A	topsoil	colluvium
	–	11–20	AB	soil (eluvial)	colluvium
	USU-3269	20–53	2Bt	soil (illuvial)	coarse colluvium
	USU-3270	53–107	2Bt2	unknown	bedrock unknown
DES12 10° headwater hillslope [PaE soil]	USU-3275	0–7	A	topsoil	colluvium
	–	7–22	AB	soil (eluvial)	colluvium
	USU-3276	22–42	B	soil (illuvial)	colluvium
	–	42–63	2Bt	soil (illuvial)	coarse colluvium
	USU-3272	63–90	2Bt2	unknown	bedrock unknown, possibly quartz dikes

with a dose rate of 0.09 Gy/s. This was followed by a 10 s 240 °C preheat and then LM-OSL from 0 to 100% LED power (max 80 mW/cm^2) over 1000 s and 250 data channels (4 s/channel) at 125 °C (Table S2). The signal was detected with a photomultiplier tube through a 7 mm Hoya U-340 filter. Signals from two blank disks were used for background subtraction from the small-aliquot LM-OSL curves. The fast-component was determined to deplete during the first 0–12% of LED intensity (0–10 mW/cm^2) as identified by Fit_LMOSL from the *Luminescence* R package (Fig. 2). Table S3 compares the fast-component intensity from the upper-most sample at each site, and the ratio of the maximum fast-component intensity to the maximum intensity from the whole LM-OSL curve. Small-aliquot LM-OSL signals are considered to be dominated by the fast-component when this ratio is greater than 50%.

A preliminary test on laboratory sensitization using CW-OSL and LM_OSL was performed on the upper-most and lower-most core samples (DUW1: USU-3056, USU-3058; DESR W1: USU-3059, USU-3061). For this test, two aliquots per sample were run through three dose-heat-bleach cycles, similar to the CW-OSL and LM-OSL methods outlined above, except LM-OSL measurements were made over 500 s, and an infrared stimulation was given prior to the OSL measurements (Fig. S2).

Single-grain LM-OSL measurements were performed on 18 samples (six samples each from soil pits DES8 and DES9 and three samples each from cores DU-W1 and DESR-W1), following the methods of Sawakuchi et al. (2011) (Table S2). Individual quartz grains were loaded into single-grain disks, which contain 100 350-μm diameter holes, a microscope was used to check that only one grain occupied each sample hole. First the natural (burial dose) signal was measured using a solid-state diode pumped green laser (532 nm) at 90% power and 125 °C (45 W/cm^2; Duller et al., 1999) for 1 s, collected over 50 data points. This measurement resets or clears out the geologic dose and stored luminescence energy. The disk of 100 quartz grains was irradiated to deliver ~100 Gy per grain. The LM-OSL measurement was conducted on each grain at 125 °C from 0 to 100% laser power (0–50 W/cm^2) linearly increased over 10 s and collected into 50 data points (0.2 s/data channel). At least 400 measurements (4 disks) were run on each sample, the same LM-OSL measurements were conducted on blank single-grain disks to allow for background correction.

3.4. Single-grain LM OSL calculations

The LM-OSL signals of the grains were analyzed to assess the percentage of grains having a total signal (area under the curve) three standard deviations greater than background (following Sawakuchi et al., 2011). The luminescence signal in photon counts per second was integrated with the trapezoidal rule to find the area under the shine down curve and estimate the integral. The integral of each LM-OSL curve was calculated by first applying the formula (eq. (1)) to each 0.2 s interval to calculate individual trapezoids under the curve:

$$\int_a^b f(x)d(x) \approx (b-a)\cdot\frac{f(a)+f(b)}{2}, \quad (1)$$

where $f(x)$ is the time between measurements and $d(x)$ is the average of the photon counts between time a and time b (0.2 s). The sum of the individual trapezoids was used to calculate the total area under the LM-OSL glow curve (total sensitivity) from 0 to 10 s of stimulation (data channels: $k = 1$ to $N = 50$):

$$\int_a^b f(x)d(x) \approx \sum_{k=1}^{N}\frac{f(xk=1)+f(xk)}{2}\Delta x_k. \quad (2)$$

We also calculated the number of 'bright' grains that have greater than 50% of their signal contained in the first 0–2 out of 10 s. The 'fast' decay is defined here as the signal between 0 and 2 s, channels 1–10, and green laser stimulation power 0–20% (0–10 W/cm^2). The 'medium'

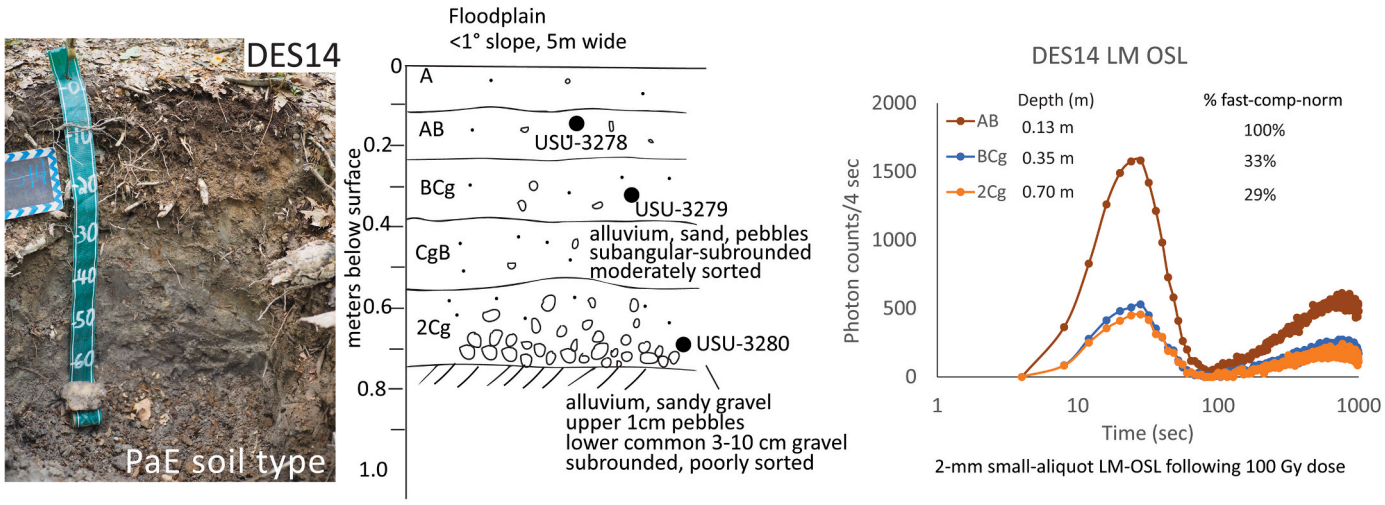

Fig. 3. Floodplain soil pit location DES14. Photo of hand-dug pit, sketch of soil stratigraphy and 2-mm small-aliquot results (average of 4 aliquots per sample). Percent fast component-normalized is maximum intensity in photon counts for first 0–12% LED power (fast-region as determined by Risø calibration sample in Fig. 2), relative to upper-most sample from site (AB horizon). Details in Table S3.

decay is defined here as the signal between 2.2 and 6 s, channels 11–30, green laser stimulation power 20–60% LED power (10–30 W/cm^2). The 'slow' decay is defined here as the signal between 6.2 and 10 s, channels 31–50, green laser stimulation power 60–100% (30–50 W/cm^2). Grains are deemed fast-dominated when 50% of the total signal is measured in the first 0–2 s of LM-OSL stimulation.

4. Results

OSL samples were collected from six sample pits dug into soils developed within a variety of parent materials (alluvium, colluvium, saprolite) and hillslope gradients and positions (Table 1). We test our hypotheses related to differing luminescence sensitivity and component intensities between allochthonous (transported) and autochthonous (produced *in situ*) material in the highly-weathered critical zone materials blanketing the Piedmont of southwestern North Carolina. We describe the small-aliquot LM-OSL results first, then follow up with more detailed single-grain LM-OSL from two soil pits and the drill cores.

4.1. Small-aliquot LM-OSL results

DES14 is a 70 cm deep soil pit located on the floodplain of a first-order tributary to the South Fork of the Catawba River (Figs. 1 and 3). The parent material is alluvium and the overlying A and B soil horizons formed within the upper of two sedimentologically distinct alluvial floodplain deposits (Cg and 2Cg). There is clast-supported gravel present in the basal unit (2Cg) and the overlying alluvial deposit is finer-grained with less gravel in the matrix sediment. The gleyed color of the lower horizons indicate water saturation conditions and a reducing environment. The upper A and AB horizons are likely bioturbated by small organisms compared to lower gravel-rich units given the finer texture and less soil moisture. Based on the landscape position and parent material, the quartz sand in these deposits is expected to have been transported through surficial (fluvial) processes. We therefore consider the samples from DES14 (USU-3278, -3279, −3280) to be a reference point example of allochthonous material in this area. The LM-OSL data show a fast-component sensitivity in all three samples, up to 70 cm depth. The intensity of the fast component is greatest in the shallow-most horizon samples (AB), while the fast-component from the lower two samples are <35% of the upper sample (Fig. 3; Table S3). All three OSL samples from DES14 have maximum intensities in the first 0–12% of LED power suggesting that their signals are dominated by the fast-component. Thus, this transported alluvial material has a moderate degree of fast-component sensitivity, while the topsoil (A horizon) exhibits stronger luminescence sensitivity likely due to bioturbation.

Five hillslope soil pits are organized in Fig. 4 in the order they are discussed below focusing first on pits with no visible saprolite. Field indicators for saprolite include zones of soft material showing foliation similar to that expected within the bedrock and 3–30 cm diameter clasts of saprolite in massive-matrix material (mobile regolith) as well as weathered intact foliated bedrock at the base of the pits (Fig. 4B). Saprolite is not apparent in the soil pits from shallow-slope locations, while it is visible in the pits around 80 cm depth for DES13, DES9, DES8 (PaD2 and PaE soil types).

Soil pits DUS2 and DES12 have very similar soil properties even though they are from different soil types (PaE and CeB2 respectively). These two soil pits are located along 10° hillslopes and the soil pits lack clear and distinct bedrock foliation at the base of the profile. The upper A soil horizons (5–7 cm depth) within these pits both have a strong fast-component (~1600–1650 photon counts max intensity). Interestingly, there is a stark contrast in the intensity of the fast component from the middle samples, both at 0.33 m depth. At site DES12, the B soil horizon fast-component intensity 1369 photon counts per 4 s, or about 85% relative to the overlying A horizon. The middle sample from DUS2 at 0.33 m depth is from a 2Bt that has 24% intensity relative to the overlying A horizon (396 counts per 4 s, USU-3269). The lower 2Bt2 horizons of both shallow-slope pits show very weak fast component, only 1–4% of the fast-component intensity relative to the upper sample at each site (Fig. 4A, Table S3). Due to the lack of sensitization of the fast-component, the lower-most units in these soil pits are suspected to be weathered saprolite, or autochthonous material that has not been to the soil surface. We interpret that sand-sized quartz grains within these units have not been transported as part of the mobile regolith nor have they been bioturbated or sensitized by *in situ* chemical weathering. The overlying Bt horizons in both pits may also act as a barrier to bioturbation and prevent mixing below this horizon. In the upper 2Bt horizon of DUS2 with a modest OSL fast component, there is a remnant of a ~80° plunging quartz vein suggesting that this horizon also derives primarily from *in situ* bedrock. The presence of a fast-component sensitized luminescence signal suggests that of some sand grains have been translocated into the upper ~30 cm of the soil (i.e. USU-3276 in pit DES12). The overall clay content of the soil likely precludes further infiltration by large grains deeper into the profile. Thus, we infer that in some cases, while chemical (and physical) weathering can be high enough to produce saprolite and remove original bedrock foliation, grains are not sensitized by this *in situ* weathering deeper in the soil

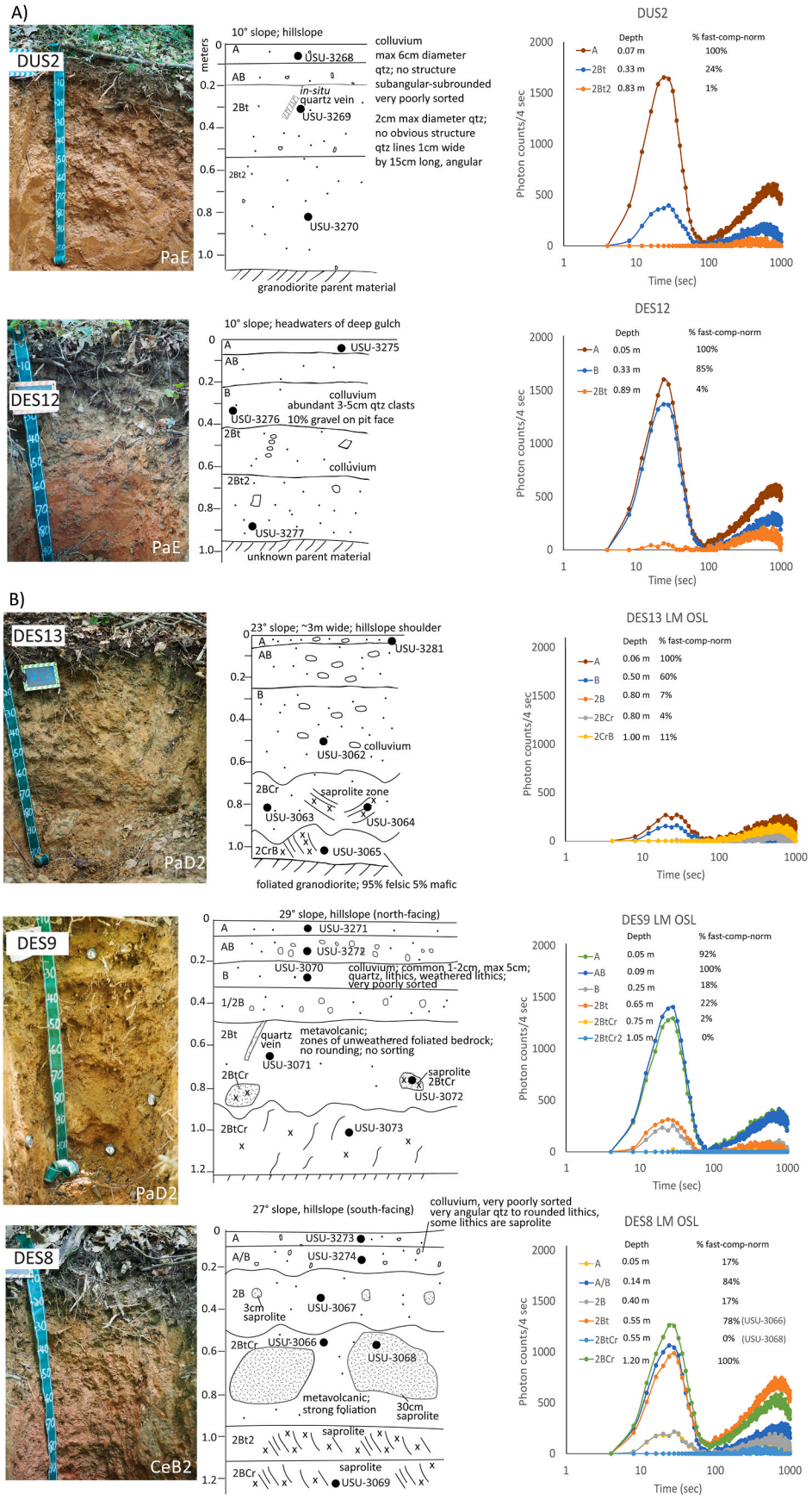

Fig. 4. Hillslope soil pits for A: DUS2, DES12, B: DES13, DES9, DES8. Photo, field sketch, 2-mm small-aliquot LM-OSL results. Small-aliquot results are average of four aliquots per sample. Percent fast component-normalized is maximum intensity in photon counts for first 0–12% LED power (fast-region as determined by calibration sample in Fig. 2), relative to upper-most sample from each site (A horizon). Details in Table S3.

profile, unlike the findings of Jeong and Choi (2012). In contrast, higher in the profile some grains may become sensitized through transport as colluvium, or with frequent visits to the surface through bioturbation (i.e. Heimsath et al., 2002).

The soil pit at DES13 is located on a hillslope shoulder with a slope angle of about 23°. The small-aliquot LM-OSL from samples in this pit have much lower fast-component intensity in the upper (A) soil horizon compared to other pit samples from similar horizons (Fig. 4B). The 2BCr soil horizon around 0.8 m depth contains two samples that were 1) collected from a foliated zone of saprolite (USU-3064) and 2) the non-foliated matrix surrounding this zone (USU-3063). In other words, the horizon between 65 and 90 cm depth contains discontinuous pockets of foliated saprolite within a non-foliated matrix. The LM-OSL results from these two samples are indistinguishable and have no sensitized fast component (Fig. 4B), or 4–7% intensity relative to the upper A horizon which is is also characterized by low luminescence sensitivity (Table S3), suggesting heterogenous weathering intensity within a single soil horizon.

Soil pit DES9 is north-facing and located on a 29° slope, the steepest in this study. The small-aliquot LM-OSL results demonstrate a sensitized fast-component in the upper A and B horizons between 0.05 and 0.65 m depth, and no fast-component sensitivity in the saprolite samples collected at 0.75 and 1.05 m depth (USU-3072 clasts in 2BtCr and USU-3073 in 2BtCr2; 0–2% fast-component intensity compared to the upper sample; Fig. 4B; Table S3). A notable difference from the previous pair of saprolite-matrix samples in DES13 at a similar depth (0.8 m) is that in DES9, the matrix surrounding saprolite clasts (regolith, 2Bt) has a small amount of fast-component sensitization (USU-3071) that is similar in magnitude to the overlying B horizon (USU-3070), 22% and 18% of the A horizon fast-component intensity respectively, and similar to the ~0.3 m depth 2Bt horizon of DUS2 which contained an intact quartz vein.

Soil pit DES8 is on a 27° south-facing slope across the gully from DES9. Given the similar landscape position, bedrock, vegetation and slope angle, DES8 is expected to show similar trends in LM-OSL sensitivity. However, the deepest sample in this soil profile was collected from a horizon with visible foliation in most areas (USU-3069 at 1.2 m depth) though it has grains with a sensitized fast component like the A/B horizon. This sensitivity is highly variable and when two bright aliquots are removed from analysis, the LM OSL curve looks more like other saprolite samples (Figure S1; Table S3). USU-3068, collected from the center of a 30 cm clast of saprolite, ~60 cm above the basal saprolite, has no sensitized fast component. Therefore, at shallower depths quartz grains within saprolite clasts are not sensitized, while deeper horizons have some grains that are sensitized.

There are three soil horizons (A, A/B, 2B) above sample USU-3068 at 50 cm depth in DES8. The middle horizon A/B is highly sensitized in the

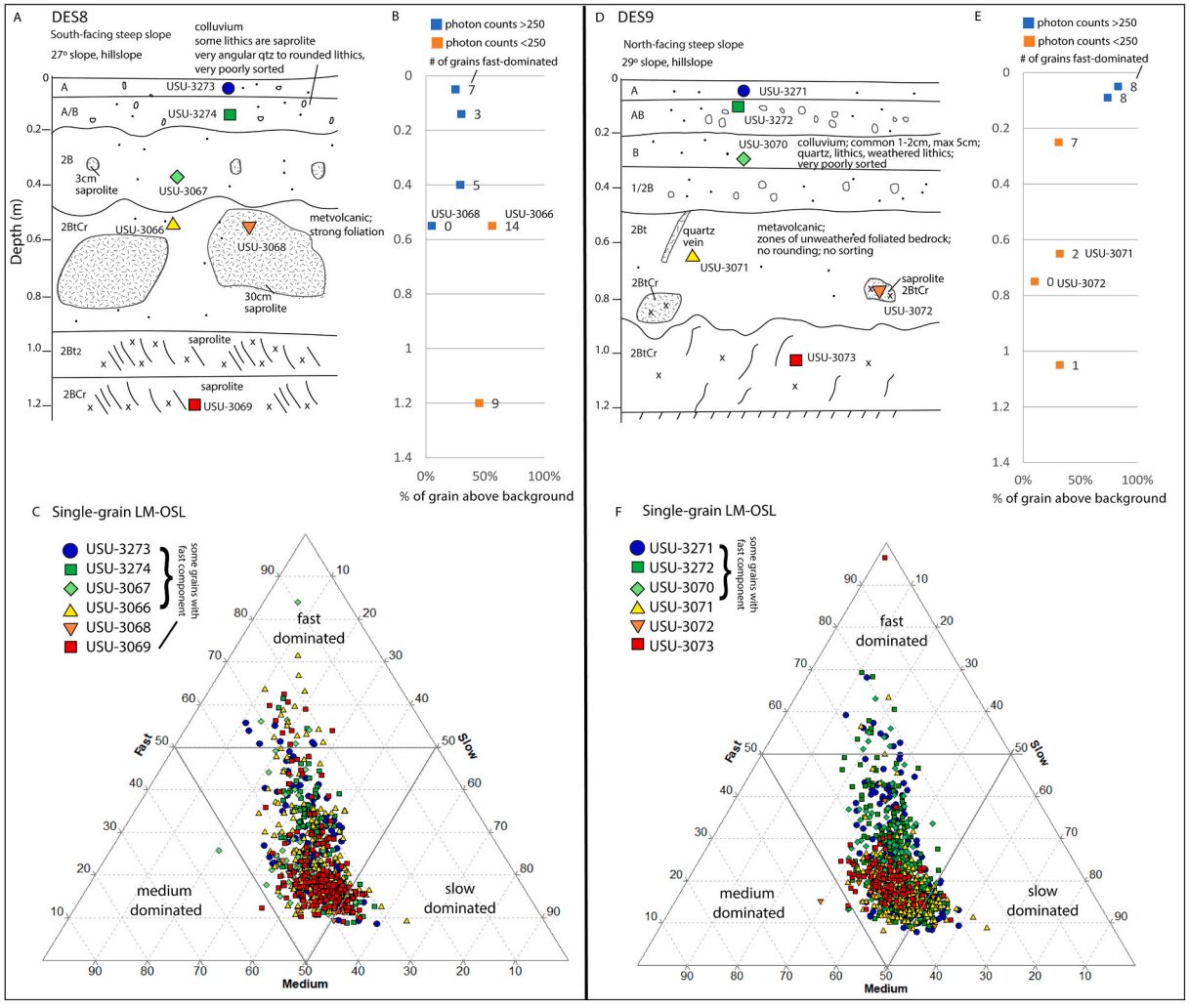

Fig. 5. Single-grain LM-OSL results from DES8 (A–C) and DES9 (D–F) soil pits. B and E plots show percent of grains above background plotted by depth. Color of square represents total signal intensity, blue for >250 photon counts and orange for <250 photon counts. Number next to data point is the number of grains with >50% of signal from the 0–2 s out of 10 s of LM-OSL measurement (fast-dominated). C and F are ternary diagrams displaying fast, medium and slow components of the SG LM-OSL signal.

fast component, while A and 2B are sensitized to a lesser degree (Fig. 4B; Table S3). The variability in sensitivity may indicate that significant vertical mixing and/or lateral transport is occurring in this exposure as there is no consistent trend with depth in the sensitivity of the fast component. The upward desensitization trend may also be a sign of vertical or lateral mixing: 1) either saprolitic grains brought up into the A and 2B horizons, and surface grains brought down into the A/B and 2BCr horizons. Or alternatively, and more plausible given the strong horizonation and layering 2) large solid clasts of local bedrock are mobilized as colluvium down the hillslope, weather to a saprolite consistency in place, and then provide a source for unsensitized grains when sampled as 'sand'. The other large saprolotized clasts in this and several other profiles support the latter. In other words, the OSL provides evidence for buried colluvial deposits as surface and near-surface samples have less sensitivity while deeper matrix samples have strong fast-component sensitivity, likely from prior colluvial transport of sensitized grains. Given the complexity of small-aliquot sensitivity in the DES8 pit, we explore the LM-OSL signals of samples from DES8 and DES9 on a more detailed level with measurements made on single quartz sand grains (Fig. 5).

4.2. Single-grain LM-OSL results

Individual sand grain LM-OSL results from soil pits DES8 and DES9 show a large variability from 5% to 83% of grains that have a bright signal (>3SD of background) (Table 2). Generally, a larger percentage of bright grains are found in the upper soil horizons, while only a small number of these bright grains have greater than 50% of the total signal from the 'fast-decay' component (Fig. 5). The south-facing steep hillslope soil pit (DES8) has fast-dominated signals for all but one LM-OSL sample, including the lowest most 2BCr saprolitic unit. The presence of these grains confirms the results seen in the small-aliquot LM-OSL curves for USU-3069 with a strong fast-component in two out of four aliquots. For the north-facing soil pit (DES9), sensitized, fast-decay dominated grains are largely restricted to the upper A and B horizons, although some sensitized grains are observed deeper into the profile. Taking what we have observed in DES8 and DES9 soil pits, we utilize the same method on core samples from interfluve landscape positions and no vertical exposure (DESR-W1 and DU-W1).

The 10 cm diameter core samples lack lateral soil pit context and a framework with overlying and underlying stratigraphy (Fig. 6). Additionally, they are clay-rich and original foliation and texture is largely absent for all but USU-3058 (24 m depth, DU-W1 core; Fig. 6). Given this ambiguity, it was difficult to discern weathered saprolite from well-developed soil through soil-core descriptions alone, particularly for the middle-depth core samples USU-3057 and USU-3060 (Fig. 6). Nevertheless, using LM-OSL, there is a clear distinction that at 5.8 m and 16 m (USU-3057 and USU-3060 respectively), as the samples have no fast decaying luminescence signal (Fig. 6). For both the small-aliquot and single-grain LM-OSL results, the core samples show a progression from low sensitivity and non-fast dominated luminescence signals at depth to more sensitive signals and increasing dominance of the fast-components from sand in the overlying clay-rich soils (Table S3, Figure S2). Notably, DU-W1 has a greater number of sensitive and fast-dominated grains (n = 40) in the upper soil sample compared to DESR-W1 (n = 3) (Table 3).

One interesting feature of the small-aliquot LM-OSL data is the lack of increased sensitization in the soil samples after three measurement cycles compared to the lowest saprolite samples (Figure S2). The LM-OSL and CW-OSL consistently show that saprolite samples have increasing fast-component sensitivity after the first beta dose-heat-optical measurement cycle. This appears more prominent in the DESR core. Differences in saprolite luminescence characteristics and sensitization are possibly due to different parent mineralogy and crystallization conditions (potentially similar to findings by Preusser et al., 2006). The lower-most samples in each of the cores are lithologically different parent materials. For USU-3061 in core DESR-W1, the saprolite is fine-textured and bedrock is metavolcanic. The saprolite sample from DU-W1 (USU-3058) is formed in coarse-textured metagranitic parent material. More work on the influence of the parent material on the luminescence properties is warranted.

5. Discussion

Floodplain and hillslope soil profiles were investigated for soil, regolith and saprolite luminescence characteristics. In general, we found that the LM-OSL signals from upper soil horizons had quartz with greater sensitivity and a higher intensity fast-decay OSL component than samples from saprolite and the interior of saprolotized clasts, which were dominated by medium and slow decay quartz signals. The observations from individual soil pits that highlight these interpretations and hypotheses of the factors that lead to these patterns are described below.

We found that soil pits on shallow slopes (DUS2 and DES12, 10° slopes) generally lack clear and distinct 'tell-tale' bedrock foliation in lower fine-textured horizons to indicate if they have weathered from *in situ* bedrock or transported sediment. The lowest horizons (2Bt) in both pits, however, show no sensitization of a fast OSL component. These horizons are likely *in situ* weathered bedrock and we infer that sand-sized quartz grains within these units have not been transported as part of the mobile regolith (colluvium) or through bioturbation, nor have they been sensitized by *in situ* chemical weathering. This may indicate that while chemical (and physical) weathering has progressed sufficiently to remove the original bedrock foliation, the grains were not sensitized by this*in situ* weathering at depths as shallow as ~0.8 m. These soil profiles therefore represent what would be typically interpreted for the Piedmont as *in situ*, weathering profiles forming in bedrock parent materials.

LM-OSL results from steep hillslope soil pit DES13 (23° slope) only

Table 2
Single-grain LM-OSL data for DES8 and DES9.

USU-#	Depth (m)	Soil description	# bright grains	# grains run	% bright grains	Average integral	2SE	# grains w/fast comp. >50%
DES-8 – South facing								
USU-3273	0.05	A	124	500	25%	333	49	7
USU-3274	0.14	A/B	121	400	30%	293	32	3
USU-3067	0.40	2B (matrix)	86	300	29%	347	70	5
USU-3066	0.55	2BtCr	223	400	56%	178	14	14
USU-3068	0.55	2BtCr (saprolite clast)	20	400	5%	409	155	0
USU-3069	1.20	2BCr	180	400	45%	201	32	9
DES-9 – North facing								
USU-3271	0.05	A	248	300	83%	298	39	8
USU-3272	0.09	AB	295	400	74%	254	32	8
USU-3070	0.25	B	157	500	31%	169.0	13	7
USU-3071	0.65	2Bt	222	700	32%	152.7	10	2
USU-3072	0.75	2BtCr (saprolite clast)	30	300	10%	165.9	22	0
USU-3073	1.05	2BtCr2	96	300	32%	160.1	18	1

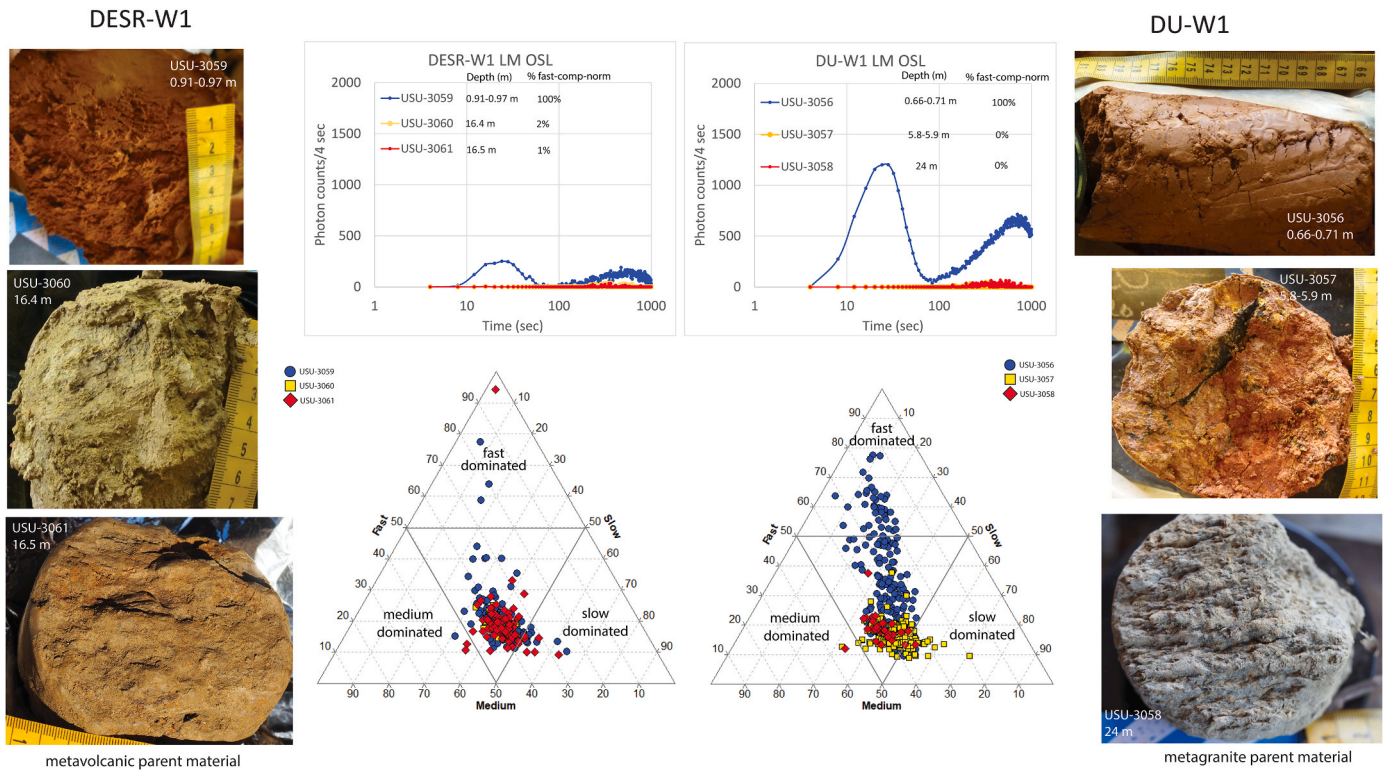

Fig. 6. DESR-W1 and DU-W1 soil and saprolite samples. 2-mm small aliquot LM-OSL results (top), ternary diagrams of single grain LM-OSL component analysis (bottom).

Table 3
Single-grain LM-OSL data for DESR-W1 and DU-W1.

USU-#	Depth (m)	# bright grains	# grains run	% bright grains	Average integral	2SE	# grains w/fast comp. >50%
DESR-W1							
USU-3059	0.91–0.97	137	400	34%	201	27	3
USU-3060	16.4	9	300	3%	354	111	0
USU-3061	16.5	93	400	23%	167	18	1
DU-W1							
USU-3056	0.66–0.71	215	400	54%	346	44	40
USU-3057	5.8–5.9	147	400	37%	135	6	0
USU-3058	24	37	400	9%	238	57	0

exhibits a sensitized fast-component within quartz sand grains in the upper two soil horizons (A and B horizon, 0–0.65 m). Deeper soil horizons composed of adjacent 'matrix' with no remaining evidence of bedrock structure (USU-3063) and zones of saprolite with visible foliation (USU-3064) and underlying intact saprolite (USU-3065) (Fig. 4), have weak small-aliquot LM-OSL signals, indicating the absence of a sensitized fast-component in grains deeper than about 65 cm. This suggests that all portions of these horizons are likely *in situ* weathered bedrock given the lack of sensitization of a fast component (similar to lower-most units from DUS2 and DES12 pits). For DES13, DUS2, and DES12 (29° vs 10° slopes), only the upper A and B horizons show clear signs of luminescence sensitization, therefore transported material overlies *in situ* bedrock in pits from these shallow and steep slopes. When comparing the intensity of the fast-component in these upper samples, we see that the samples from the steeper slope (DES13) have much lower intensity, particularly the A horizon by about two-thirds compared to the lower-slope pits (Fig. 4). This difference is consistent with the difference in the assumed residence time of the two profiles – as suggested by the much greater degree of overall weathering (redness, clay content, soil structure) of the DUS2 and DES12 pits compared to the steeper hillslope setting of the DES13 pit. The weaker soil development in the DES13 pit provides evidence that the erosion rate and rate of passage of colluvium into and out of the hillslope position at that site is faster than the shallower and possibly more stable slopes of DUS2 and DES12. In other words, we are interpreting that sand grains in the A and B horizons at DES13 are less sensitive to luminescence due to the shorter residence time in the hillslope soil and as mobile regolith. Additionally, the higher sensitivity, particularly noted in the intensity of the fast component, in quartz sand grains from the A and B horizons at DUS2 and DES12 may be also due to a longer period of *in situ* bioturbation in the upper 0–~35 cm, above the lowest sampled horizon. Again, the much greater degree of overall weathering in these upper horizons is consistent with longer exposure durations and more stable hillslopes at these two sites.

Two additional hillslope soil pits (DES9-north-facing and DES8-south-facing) have basal horizons with mostly continuous foliated saprolite. Saprolite clasts (~3–30 cm in diameter) overlie the basal saprolite layers in both soil profiles. The clast interiors lack a sensitive fast-component, while the matrix surrounding the clasts contain sensitized quartz sand. These results suggest that the isolated saprolite clasts and matrix may have experienced transport and incorporation of grains from the surface and/or grains from higher soil horizons. These results suggest that the saprolite clasts likely represent mobile regolith that was transported from up-slope along this steep tributary hillslope. Therefore, while the interiors of the clasts themselves are not sensitized, the matrix

surrounding the clasts appear to have been derived from pedogenic soil horizons containing sensitized grains.

Results from DES9 shows a lack of sensitization in the deep saprolitic units. For DES8, however, the deepest sample (USU-3069) was collected from a highly weathered saprolite (2BtCr) at 1.2 m. This sample has an unusually high number of bright grains (45%; 9 grains with dominant fast component). These results provide more detail on the past mixing processes at the site than can be inferred from field data alone. The high proportion of sensitized grains in this sample suggests mixing of grains from higher in the profile into the saprolite through soil processes consistent with the field observation of translocated clays at this depth in DES8 (2BtCr) versus DES9 (2BCr). One observation is that DES8 was dug into soil type PaE which contains <20% clay, while DES9 is in a sandy clay loam (PaD2) which contains 20–40% clay (Natural Resources Conservation Service, 2019). It is possible that grains are transported deeper within a blocky ped structure soil (DES8-PaE) than a platy soil (DES9-PaD2), which tends to inhibit wide cracks and conduits for particle and water movement. Another factor that may impact the soil mixing and down-slope transportation processes between these two soil pits is the difference in the hillslope aspect. Further investigation is needed to determine why translocation of sensitized (surface) grains is deeper for the south-facing hillslope site.

Small-aliquot and single-grain LM-OSL from soil core samples at summit and interfluve locations show similar trends to the soil pits. Deep samples have little to no luminescence sensitivity while the upper soil is sensitized with peak intensity of the fast component ranging from 250 to 1250 photon counts per 100 Gy (like the soil pit A horizons). The variability in the intensity of the fast-component in the upper soil samples might suggest that landscape position and soil type (CeB2) are not major factors affecting the sensitization of *in situ* quartz for interfluve and summit sites. One major difference between the two core sites is the parent material. Across the five hillslope soil pit sites, all likely formed over metavolcanic bedrock except DES13 which has a granodiorite parent material. The soil pits with underlying metavolcanic parent material have stronger LM-OSL fast-component sensitivity, while the granodiorite (DES13) is the least sensitive. Lithology may be a contributing factor to luminescence sensitivity as seen in other studies (e.g. Preusser et al., 2006; Sawakuchi et al., 2011; Jeong and Choi, 2012), but the degree to which this controls *in situ* sensitization is not clear. DESR-W1 parent material is metavolcanic and has a finer texture than DU-W1 which has metagranitic parent material and is coarser textured. However, the upper soil sample (USU-3059) from DESR-W1 is less sensitive than DU-W1 (USU-3056). If parent material is a contributing factor to luminescence sensitivity, then DESR-W1 *in situ* soil should have greater luminescence sensitivity than DU-W1 based on the soil pit data. Given the opposite case for these two core sites, we hypothesize that the DU-W1 upper soil sample has allochthonous quartz sand input, possibly from eolian contribution given the interfluve landscape position. Alternatively, this field site could also represent an area of inverted topography similar to that observed in other major interfluves in the Piedmont (e.g. Ferguson et al., 2019). The similarity between the photon counts/sensitivity of the upper portion of this soil and that of our definitive transported sediment from other locations within the field site supports the idea that the upper sediments of this interfluve are paleocolluvial or paleoalluvial sediments.

6. Conclusions

Identifying unique depositional packages of surface sediments is a foundational component of geomorphic research and is key to understanding landscape evolution processes and history. Yet, in the highly weathered soils of the Piedmont region of the southeastern USA, transported sediment versus *in situ* weathered bedrock are difficult to distinguish in the field due to their similar character and appearance after intense weathering has removed primary bedrock structures like foliation. Previous luminescence sampling in soils have focused on quantifying soil processes through dose distributions and apparent ages. Our work is distinguished from these previous studies because we present small-aliquot and single-grain linear modulated OSL from quartz sand grains in soil and saprolite samples that track the sensitization of quartz in the critical zone. Results from this study indicate that luminescence sensitivity can be a useful tool to identify and differentiate between transported sediments and *in situ* weathered bedrock, even when they are highly weathered. Luminescence signal components derived from small-aliquot and single-grain LM-OSL analyses indicate that upper soil horizons forming in colluvium (A and B horizons, 0–20 cm depth) have the greatest luminescence sensitivity, and contain proportions of sensitive quartz grains (5–20%) that are dominated by the fast-decaying component. These observations suggest that surface process that sensitize grains through repeated cycles of exposure to light and radiation generated these luminescence properties in the active upper soil horizons. Saprolite and the interior of saprolitic clasts have low sensitivity and weak to no fast-component intensity. In some cases, the 'matrix' surrounding the saprolitic clasts and foliated zones of saprolite are sensitive to luminescence and contain a fast-component, but not in all cases. Thus, we conclude that colluvium (mobile regolith) can be distinguished from saprolite lacking original rock fabric based on the LM-OSL sensitivity and fast component intensity. Grains from upper soil horizons (A and B) can be translocated and mixed into saprolite at depth can be identified with SG-LM-OSL but seem to coincide with evidence of translocated clay as well. The use of LM-OSL is an important tool to differentiate between similar appearing, highly weathered soils developed within transported sediment and *in situ* weathered bedrock and saprolite.

Funding

This research did not receive any specific grant from funding agencies in the public, commercial, or not-for-profit sectors.

Declaration of competing interest

The authors declare that they have no known competing financial interests or personal relationships that could have appeared to influence the work reported in this paper.

Acknowledgements

We are grateful to all the people who helped make this work possible. Eppes' Applied Soil Science Class of 2019 excavated all soil pits with support from the University of North Carolina at Charlotte and the Redlair Observatory. Well drilling was supported in part through a grant provided by the Duke Energy Water Resources Fund. Ramirez, G., Smith, H., DiPietro, J. as field assistants for soil field descriptions. The technical laboratory staff at Utah State University Luminescence Laboratory who helped process and run the OSL samples: Carlie Ideker, Harriet Cornachione, and Maggie Erlick. We are thankful to our reviewer Tony Reimann whose suggestions greatly improved the layout of the manuscript, and the handling editor Regina DeWitt.

Appendix A. Supplementary data

Supplementary data to this article can be found online at https://doi.org/10.1016/j.quageo.2022.101343.

References

Aitken, M.J., 1998. An Introduction to Optical Dating: the Dating of Quaternary Sediments by the Use of Photon-Stimulated Luminescence. Oxford University Press, New York.

Anderson, R.S., Rajaram, H., Anderson, S.P., 2019. Climate driven coevolution of weathering profiles and hillslope topography generates dramatic differences in critical zone architecture. Hydrol. Process. 33 (1), 4–19.

Bailey, R.M., Smith, B.W., Rhodes, E.J., 1997. Partial bleaching and the decay form characteristics of quartz OSL. Radiat. Meas. 27 (2), 123–136.
Bateman, M.D., Frederick, C.D., Jaiswal, M.J., Singhvi, A.K., 2003. Investigations into the potential effects of pedoturbation on luminescence dating. Quat. Sci. Rev. 22, 1169–1176.
Bateman, M.D., Boulter, C.H., Carr, A.S., Frederick, C.D., Peter, D., Wilder, M., 2007. Detecting post-depositional sediment disturbance in sandy deposits using optical luminescence. Quat. Geochronol. 2, 57–64.
Brimhall Jr., G.H., Dietrich, W.E., 1987. Constitutive mass balance relations between chemical composition, volume, density, porosity, and strain in metasomatic hydrochemical systems: results on weathering and pedogenesis. Geochem. Cosmochim. Acta 51, 567–587.
Brimhall, G.H., Lewis, C.J., Ford, C., Bratt, J., Taylor, G., Warin, O., 1991. Quantitative geochemical approach to pedogenesis: importance of parent material reduction, volumetric expansion, and eolian influx in lateritization. Geoderma 50, 51–91. https://doi.org/10.1016/0016-7061(91)90066-3.
Bulur, E., Bøtter-Jensen, L., Murray, A.S., 2000. Optically stimulated luminescence from quartz measured using the linear modulation technique. Radiat. Meas. 32 (5–6), 407–411.
Duller, G.A.T., 2008. Single-grain optical dating of Quaternary sediments: why aliquot size matters in luminescence dating. Boreas 37, 589–612.
Duller, G.A.T., Bøtter-Jensen, L., Murray, A.S., Truscott, A.J., 1999. Single grain laser luminescence (SGLL) measurement using a novel automated reader. Nucl. Instrum. Methods B 155, 506–514.
Durcan, J., King, G.E., Duller, G.A.T., 2015. DRAC: dose rate and age calculator for trapped charge dating. Quat. Geochronol. 28, 54–61.
Feathers, J., 2002. Luminescence dating in less than ideal conditions: case studies from Klasies river main site and Duinefontein, South Africa. J. Archaeol. Sci. 29, 177–194.
Ferguson, T.A., Bacon, A.R., Eppes, M.C., Richter, D.D., Willard, D.A., Nelson, M., Billings, S.A., Austin, J., 2019. Rethinking the development of the Piedmont uplands of southeastern north America: pleistocene age colluvium and organic-rich sediments dating from early MIS 3 to MIS 5. In: AGU Fall Meeting Abstracts EP53F-2197.
Fitzsimmons E., K., Rhodes, E.J., Barrows T., T., 2010. OSL dating of southeast Australian quartz: a preliminary assessment of luminescence characteristics and behaviour. Quat. Geochronol. 5 (2–3), 91–95. https://doi.org/10.1016/j.quageo.2009.02.009.
Forrest, B., Rink, W.J., Bicho, N., Ferring, C.R., 2003. OSL ages and possible bioturbation signals at the Upper Paleolithic site of Lagoa do Bordoal, Algarve, Portugal. Quat. Sci. Rev. 22 (10–13), 1279–1285.
Furbish, D.J., Roering, J.J., Keen-Zebert, A., Almond, P., Doane, T.H., Schumer, R., 2018. Soil particle transport and mixing near a hillslope crest: 2. Cosmogenic nuclide and optically stimulated luminescence tracers. J. Geophys. Res.: Earth Surf. 123, 1078–1093. https://doi.org/10.1029/2017JF004316.
Goldsmith, Richard, Milton, D.J., Horton Jr., J.W., 1988. Geologic Map of the Charlotte 1 Degree X 2 Degrees Quadrangle, North Carolina and South Carolina: U.S. Geological Survey, Miscellaneous Investigations Series Map I-1251-E, Scale 1:250,000.
Gosse, J.C., Phillips, F.M., 2001. Terrestrial in situ cosmogenic nuclides: theory and application. Quat. Sci. Rev. 20 (14), 1475–1560. https://doi.org/10.1016/S0277-3791(00)00171-2.
Götze, J., 2000. Cathodoluminescence microscopy and spectroscopy in applied mineralogy. Freiberg. Forschungsh. C485, 128.
Granger, D.E., Riebe, C.S., 2014. Cosmogenic nuclides in weathering and erosion. In: Drever, J.I. (Ed.). In: Turekian, K.K., Holland, H.D. (Eds.), Surface and Ground Water, Weathering and Soils, vol. 7. Elsevier-Pergamon, Oxford, pp. 401–436. Treatise on Geochemistry.
Gray, H.J., Jain, M., Sawakuchi, A.O., Mahan, S.A., Tucker, G.E., 2019. Luminescence as a sediment tracer and provenance tool. Rev. Geophys. 57 https://doi.org/10.1029/2019RG000646.
Guralnik, B., Ankjærgaard, C., Jain, M., Murray, A.S., Müller, A., Wälle, M., Lowick, S.E., Preusser, F., Rhodes, E.J., Wu, T.-S., Mathew, G., Herman, F., 2015. OSL-thermochronometry using bedrock quartz: a note of caution. Quat. Geochronol. 25, 37–48.
Guo, L., Lin, H., 2016. Critical zone research and observatories: current status and future perspectives. Vadose Zone J. 15 (9) https://doi.org/10.2136/vzj2016.06.0050.
Hansen, V., Murray, A., Buylaert, J.-P., Yeo, E.-Y., Thomsen, K., 2015. A new irradiated quartz for beta source calibration. Radiat. Meas. 81, 123–127.
Heimsath, A.M., Dietrich, W.E., Nishiizumi, K., Finkel, R.C., 1997. The soil production function and landscape equilibrium. Nature 388p, 358–361.
Heimsath, A., Chappell, J., Spooner, N.A., Questiaux, D.G., 2002. Creeping soil. Geology 30 (2), 111–114. https://doi.org/10.1130/0091-7613(2002)030<0111:CS>2.0.CO.
Heimsath, A.M., Korup, O., 2012. Quantifying rates and processes of landscape evolution. Earth Surf. Process. Landforms 37, 349-251.
Holbrook, W.S., Riebe, C.S., Elwaseif, M., Hayes, J.L., Reeder, K., Harry, D.L., Malazian, A., Dosseto, A.J., Hartsough, P.C., Hopmans, J.W., 2014. Geophysical constraints on deep weathering and water storage potential in the Southern Sierra Critical Zone Observatory. Earth Surf. Process. Landforms 39, 366–380.
Huntley, D.J., Godfrey-Smith, D.I., Thewalt, M.L.W., 1985. Optical dating of sediments. Nature 313, 105–107. https://doi.org/10.1038/313105a0.
Jeong, G.Y., Cheong, C.-S., Choi, J.-H., 2007. The effect of weathering on optically stimulated luminescence dating. Quat. Geochronol. 2, 117–122.
Jeong, G.Y., Choi, J.-H., 2012. Variations in quartz OSL components with lithology, weathering and transportation. Quat. Geochronol. 10, 320–326.
Kristensen, J.A., Thomsen, K.J., Murray, A.S., Buylaert, J.P., Jain, M., Breuning-Madsen, H., 2015. Quantification of termite bioturbation in a savannah ecosystem: application of OSL dating. Quat. Geochronol. https://doi.org/10.1016/j.quageo.2015.02.026.
Kreutzer, S., 2021. In: Kreutzer, S., Burow, C., Dietze, M., Fuchs, M.C., Schmidt, C., Fischer, M., Friedrich, J., Mercier, N., Philippe, A., Riedesel, S., Autzen, M., Mittelstrass, D., Gray, H.J. (Eds.), fit_LMCurve( ): Nonlinear Least Squares Fit for LM-OSL Curves. Function Version 0.3.3. Luminescence: Comprehensive Luminescence Dating Data Analysis. R package version 0.9.15, 2021. https://CRAN.R-project.org/package=Luminescence.
Lain B., O., Roberts G., R., 2006. Dating the quaternary: progress in luminescence dating of sediments. Quat. Sci. Rev. 25 (19–20), 2449–2468. https://doi.org/10.1016/j.quascirev.2005.11.013.
Lebedeva, M.I., Brantley, S.L., 2013. Exploring geochemical controls on weathering and erosion of convex hillslopes: beyond the empirical regolith production function. Earth Surf. Process. Landforms 38 (15), 1793–1807.
Merritts, D.J., Chadwick, O.A., Hendricks, D.M., 1991. Rates and processes of soil evolution on uplifted marine terraces, northern California. Geoderma 51, 241–275.
Moska, P., Murray, A.S., 2006. Stability of the quartz fast-component in insensitive samples. Radiat. Meas. 41, 878–885.
Munyikwa, K., 2000. Cosmic ray contribution to environmental dose rates with varying overburden thickness. Ancient TL 18 (2), 27–34.
Murray, A.S., Wintle, A.G., 2000. Luminescence dating of quartz using an improved single-aliquot regenerative-dose protocol. Radiat. Meas. 32, 57–73.
Natural Resources Conservation Service, 2019. United Stated Department of Agriculture, Web Soil Survey. Digital General Soil Map of U.S. https://websoilsurvey.sc.egov.usda.gov/app/WebSoilSurvey.aspx. (Accessed 28 April 2022)
Nelson, M., Rittenour, T., Cornachione, H., 2019. Sampling methods for luminescence dating of subsurface deposits from cores. Method Protocol. 2, 88. https://doi.org/10.3390/mps2040088.
Norton, E.A., 1939. Soil Conservation Survey Handbook (No. 352). US Department of Agriculture.
Pavich, M.J., Brown, L., Valette-Silver, J.N., Klein, J., Middleton, R., 1985. ^{10}Be analysis of a Quaternary weathering profile in the Virginia Piedmont. Geology 13, 39–42.
Pavich, M.J., 1989. Regolith residence time and the concept of surface age of the Piedmont "peneplain. Geomorphology 2, 181–196.
Pelletier, J.D., Brad Murray, A., Pierce, J.L., Bierman, P.R., Breshears, D.D., Crosby, B.T., Ellis, M., Foufoula-Georgiou, E., Heimsath, A.M., Houser, C., Lancaster, N., 2015. Forecasting the response of Earth's surface to future climatic and land use changes: a review of methods and research needs. Earth's Future 3 (7), 220–251.
Pietsch, T., Olley, J.M., Nanson, G.C, 2008. Fluvial transport as a natural luminescence sensitiser of quartz. Quat. Geochronol. 3 (4), 365–376. https://doi.org/10.1016/j.quageo.2007.12.005.
Preusser, F., Ramseyer, K., Schlüchter, C., 2006. Characterisation of low OSL intensity quartz from the New Zealand Alps. Radiat. Meas. 41, 871–877.
Reimann, T., Román-Sánchez, A., Vanwalleghem, T., Wallinga, J., 2017. Getting a grip on soil reworking – single-grain feldspar luminescence as a novel tool to quantify soil reworking rates. Quat. Geochronol. 42, 1–14. https://doi.org/10.1016/j.quageo.2017.07.002.
Rempe, D.M., Dietrich, W.E., 2014. A bottom-up control on fresh-bedrock topography under landscapes. Proc. Natl. Acad. Sci. Unit. States Am. 111 (18), 6576–6581.
Richter, D.D., Eppes, M.-C., Austin, J.C., Bacon, A.R., Billings, S.A., Brecheisen, Z., Ferguson, T.A., Markewitz, D., Pachon, J., Schroeder, P.A., Wade, A.M., 2020. Soil production and the soil geomorphology legacy of Grove Karl Gilbert. Soil Sci. Soc. Am. J. 84, 1–20. https://doi.org/10.1002/saj2.20030.
Riebe, C.S., Hahm, W.J., Brantley, S.L., 2017. Controls on deep critical zone architecture: a historical review and four testable hypotheses. Earth Surf. Process. Landforms 42, 128–156.
Rodés, Á., Evans, D., 2020. Cosmogenic soil production rate calculator. MethodsX 7, 100753.
Román-Sánchez, A., Reimann, T., Wallinga, J., Vanwalleghem, T., 2019. Bioturbation and erosion rates along the soil-hillslope conveyor belt, part 1: insights from single-grain feldspar luminescence. Earth Surf. Process. Landforms 44 (10), 2051–2065.
Sawakuchi, A.O., Blair, M.W., DeWitt, R., Faleiros, F.M., Hyppolito, T.N., Guedes, C.C.F., 2011. Thermal history versus sedimentary history: OSL sensitivity of single quartz grains extracted from igneous and metamorphic rocks and sediments. Quat. Geochronol. 6, 261–272.
Sawakuchi, A.O., Jain, M., Mineli, T.D., Nogueira, L., Bertassoli Jr., D.J., Häggi, C., Sawakuchi, H.O., Pupim, F.N., Grohmann, C.H., Chiessi, C.M., Zabel, M., Multiza, S., Mazoca, C.E.M., Cunha, D.F., 2018. Luminescence of quartz and feldspar fingerprints provenance and correlates with the source area denudation in the Amazon River basin. Earth Planet Sci. Lett. 492, 152–162.
Simkins, L.M., DeWitt, R., Simms, A.R., Briggs, S., 2016. Investigation of optically stimulated luminescence behavior of quartz from crystalline rock surfaces: a look forward. Quat. Geochronol. 36, 161–173.
Velbel, M.A., Price, J.R., 2007. Solute geochemical mass-balances and mineral weathering rates in small watersheds: methodology, recent advances, and future directions. Appl. Geochem. 22 (8), 1682–1700.
White, T., Brantley, S., Banwart, S., Chorover, J., Dietrich, W., Derry, L., Lohse, K., et al., 2015. The role of critical zone observatories in critical zone science: developments in Earth. Surface Proc. 19, 15–78.